WILEY **Journal of Molecular Recognition**

RESEARCH ARTICLE

Biophysical analysis of the dynamics of calmodulin interactions with neurogranin and Ca^{2+}/calmodulin-dependent kinase II

Christian Seeger[1,2] | Vladimir O. Talibov[1] | U. Helena Danielson[1,2,3] [iD]

[1]Department of Chemistry - BMC, Uppsala University, Uppsala, Sweden
[2]Beactica AB, Uppsala, Sweden
[3]Science for Life Laboratory, Uppsala University, Uppsala, Sweden

Correspondence
U. Helena Danielson, Department of Chemistry - BMC, Uppsala University, Box 576, SE-751 23 Uppsala, Sweden.
Email: helena.danielson@kemi.uu.se

Abstract

Calmodulin (CaM) functions depend on interactions with CaM-binding proteins, regulated by Ca^{2+}. Induced structural changes influence the affinity, kinetics, and specificities of the interactions. The dynamics of CaM interactions with neurogranin (Ng) and the CaM-binding region of Ca^{2+}/calmodulin-dependent kinase II (CaMKII$_{290-309}$) have been studied using biophysical methods. These proteins have opposite Ca^{2+} dependencies for CaM binding. Surface plasmon resonance biosensor analysis confirmed that Ca^{2+} and CaM interact very rapidly, and with moderate affinity (K_D^{SPR} = 3 μM). Calmodulin-CaMKII$_{290-309}$ interactions were only detected in the presence of Ca^{2+}, exhibiting fast kinetics and nanomolar affinity (K_D^{SPR} = 7.1 nM). The CaM–Ng interaction had higher affinity under Ca^{2+}-depleted (K_D^{SPR} = 480 nM, k_1 = 3.4 × 10^5 M^{-1} s^{-1} and k_{-1} = 1.6 × 10^{-1} s^{-1}) than Ca^{2+}-saturated conditions (K_D^{SPR} = 19 μM). The IQ motif of Ng (Ng$_{27-50}$) had similar affinity for CaM as Ng under Ca^{2+}-saturated conditions (K_D^{SPR} = 14 μM), but no interaction was seen under Ca^{2+}-depleted conditions. Microscale thermophoresis using fluorescently labeled CaM confirmed the surface plasmon resonance results qualitatively, but estimated lower affinities for the Ng (K_D^{MST} = 890 nM) and CaMKII$_{290-309}$ (K_D^{MST} = 190 nM) interactions. Although CaMKII$_{290-309}$ showed expected interaction characteristics, they may be different for full-length CaMKII. The data for full-length Ng, but not Ng$_{27-50}$, agree with the current model on Ng regulation of Ca^{2+}/CaM signaling.

KEYWORDS

calmodulin, calmodulin-dependent kinase, microscale thermophoresis, neurogranin, surface plasmon resonance

1 | INTRODUCTION

Biological processes are regulated via complex networks involving protein-protein interactions complemented by protein interactions with nucleic acids, small organic ligands, and inorganic ions. The occurrence and localization of the proteins are regulated genetically while the concentration of small organic ligands and ions can be regulated by other mechanisms. The different regulatory mechanisms influence not only the localization of the effect but also how rapid the onset of the effect is as well as its duration and specificity. To better understand biological processes, we need new strategies that do not simply identify interacting proteins and their binding partners, their structures, and localization, but that also allow the interaction mechanism, affinities, and kinetics to be determined under various conditions reflecting the dynamics and specificities of their biological environment.

Calmodulin (CaM) is involved in many protein-protein networks and thereby plays a central role in the regulation of physiological processes, including signaling and synaptic plasticity of the brain. It is regulated by variations in Ca^{2+} concentrations that influence its interactions with CaM-binding proteins (CaMBP). They include enzymes,

---

like Ca^{2+}/calmodulin-dependent protein kinase II (CaMKII), and noncatalytic proteins, like neurogranin (Ng).[1] Calmodulin interacts primarily in a Ca^{2+}-bound form, but the apo form of CaM can also interact with CaMBPs, giving CaM an active role over a broad range of Ca^{2+} concentration. The dynamics of the CaM interactome is not known as there is little information about the affinities of the interactions under different conditions and how it regulates the specificity of the interactions between CaM and CaMBPs. Here, we have devised biophysical methods that can provide both mechanistic and quantitative equilibrium-based and kinetic data, i.e., affinity (K_D) and association and dissociation rate constants (k_1 and k_{-1}).

Calmodulin belongs to the helix-loop-helix motif (EF-hand) family of Ca^{2+}-binding proteins and contains 2 pairs of canonical EF-hands that are separated by an α-helical linker.[2] Binding of Ca^{2+} to apoCaM induces a conformational change from a compact to an open form. It exposes a hydrophobic pocket in both the N- and C-terminal domains of CaM involved in interactions with a broad range of target proteins.[2-4] Most proteins, like CaMKII, interact with Ca^{2+}/CaM (open form),[5] while some proteins, like Ng and neuromodulin, have a preference toward apoCaM (compact form). [1,6-8]

Calmodulin-dependent protein kinase II is one of the major Ca^{2+} signal transducers. The protein exists in various isoforms. The kinase subunit consists of 3 functional domains (catalytic, autoinhibitory, and self-associated), assembled into dodecameric homooligomer and heterooligomer (reviewed in Lisman et al. and Hunter and Schulman[9,10]). Excluding splicing variants, CaMKII occurs in 2 isoforms, namely, α and β. They are highly enriched in the brain, especially the hippocampus.[11,12] Both isoforms contain a CaM-binding region, represented by the same polypeptide sequence (in human, aa290-300 in CaMKIIα and aa291-301 in CaMKIIβ). Calmodulin-dependent protein kinase II is a key component for induction of long-term potentiation in excitatory synapses. It acts by phosphorylation of Ser831 in GluA1-containing α-amino-3-hydroxy-5-methyl-4-isoxazole propionic acid receptors (AMPA receptors), thereby increasing single-channel conductance.[13] Furthermore, CaMKII leads to increased insertion of AMPA receptors into the postsynaptic membrane, which further increases synaptic strength.[1] The interaction between Ca^{2+}/CaM and CaMKII leads to autophosphorylation and activation of the enzyme, which remains active even after it dissociates from Ca^{2+}/CaM.[14]

Neurogranin, together with neuromodulin and pep19, belongs to the calpacitin group of proteins that is primarily found in neurons. Expression of Ng has been shown to correlate with the onset of synaptogenesis in rats and mice in brain regions that display high levels of neuroplasticity, like the hippocampus.[15] Neurogranin has a molecular

weight of 7.8 kDa and has a sequence similar to neuromodulin in a region spanning 20 amino acids that contains an IQ motif (I/L/V)QXXXRXXXX(R/K)XX(F/I/L/V/W/Y).[16] It corresponds to the protein kinase C phosphorylation and CaM-binding site.[6,7] It has been shown that the interaction between Ng and CaM enhances synaptic strength.[17] Recent data suggest that Ng slows down the diffusion of CaM and increases its concentration at dendritic spines, which, in turn, leads to enhanced Ca^{2+} sensitivity in the synapse.[18]

Proteins that are regulated by CaM display different levels of Ca^{2+} sensitivity. This is achieved by cooperativity between the CaM-CaMBP complexes and the binding of Ca^{2+}. Positive cooperativity, characterized by an increase of Ca^{2+} affinity upon protein binding to calmodulin, has been described for the CaM-troponin I and the CaM-CaMKII complexes.[19-21] An opposing effect on the affinity for Ca^{2+} to CaM has been observed for the CaM/Ng complex.[8,21] The modulation of CaM by different protein targets has recently been described according to the allosteric transition model of Monod, Wyman, and Changeux.[22,23]

To better understand how CaM exerts its physiological effect, we were interested in developing informative assays that could provide information on the dynamics of the interactions between CaM and CaMBPs, and how the interactions are influenced by Ca^{2+}. We have previously used surface plasmon resonance (SPR) biosensor technology to distinguish the characteristics of the interactions of CaM and caldendrin with the scaffolding protein, AKAP79.[24,25] These studies revealed that although there were only minor differences in affinity,
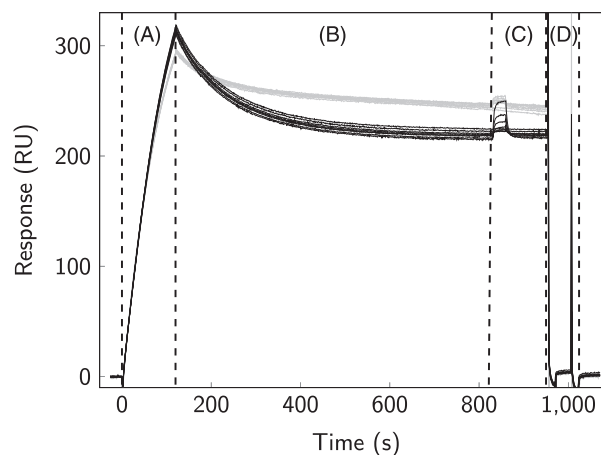

FIGURE 2 Assay setup for SPR-based interaction studies between immobilized Ng$_{fl}$ and CaM. A, affinity capture of Ng$_{fl}$ to SPR biosensor surfaces by covalently immobilized polyhistidine antibody; B, stabilization period; C, injection of CaM under Ca^{2+}-saturated (gray) and Ca^{2+}-depleted conditions (black); D, surface regeneration

FIGURE 1 Primary structures of the studied polypeptides. The EF-hand pairs of human calmodulin (CaM) (P62158) are highlighted (EF-1 and EF-2 in blue, EF-3 and EF-4 in green). The IQ motif of human neurogranin (Ng) (Q92686) is underlined

the interaction mechanisms translated into different kinetics and Ca^{2+}-dependencies, presumably leading to different functions in the synapse.

The interaction between CaM and Ng has been characterized in 2 independent studies by using isothermal titration calorimetry (ITC). They showed that Ng binds to CaM with nanomolar affinity in the absence and with low micromolar affinity in the presence[6,8] of Ca^{2+}. The present study aimed to shed additional light on this interaction by a time-resolved approach using SPR biosensor analysis.

To supplement SPR experiments, we used microscale thermophoresis (MST) analysis as an orthogonal equilibrium-based method to study CaM interactions. The technique is based on the motions of molecules and dispersed particles in a temperature gradient.[26]

Since thermodiffusion depends on the particle-solvent interface, which changes upon a binding event, monitoring the dose-response dependency of particles mobility allows the determination of equilibrium dissociation constant (K_D).[27] Another solution-based label-free method, UV fluorescence spectroscopy, was used as a third strategy to study the interactions between Ca^{2+} and CaM, validating the functionality of the designed assays. This method is commonly used for studies of CaM and monitors the changes in intrinsic tyrosine fluorescence in CaM upon Ca^{2+}-induced conformational changes.[4,28,29]

For the present study, we used a peptide of CaMKII including the CaM-binding site ($CaMKII_{290-309}$), and both full-length Ng (Ng_{fl}) and Ng-derived peptide containing an IQ motif (Ng_{27-50}, Figure 1).
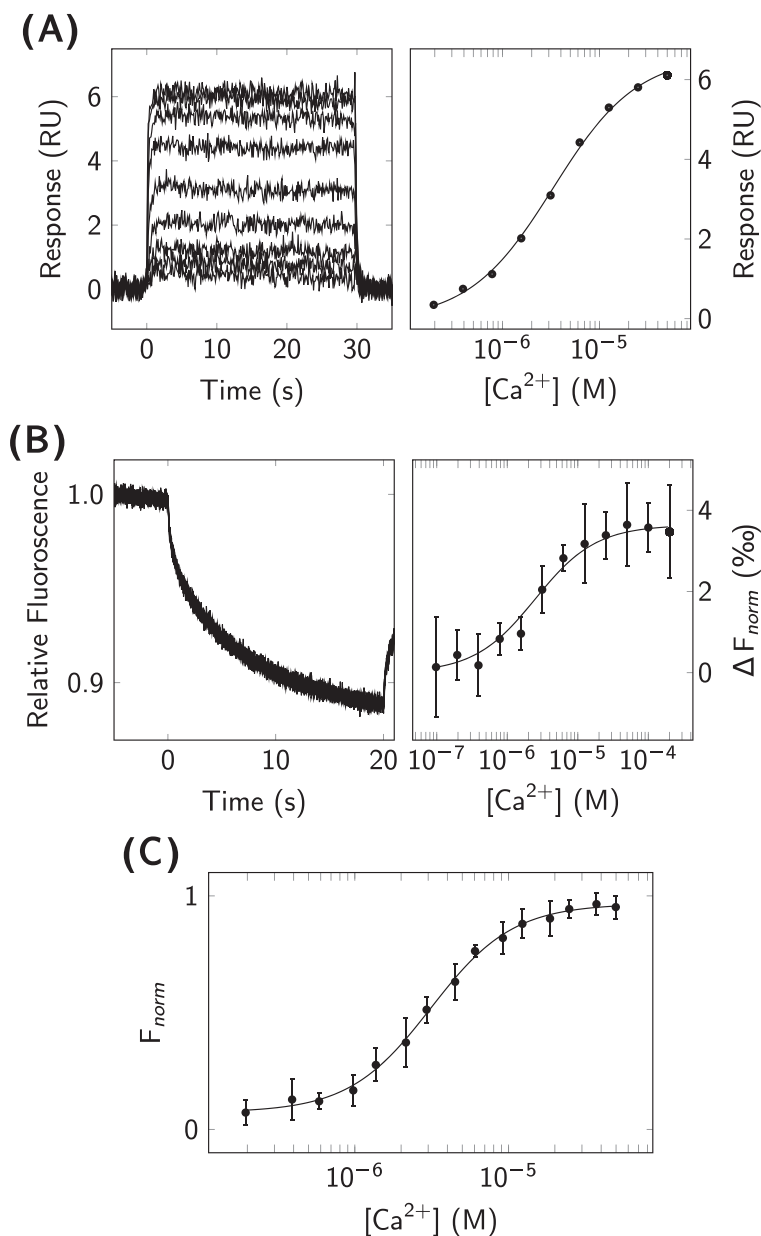

FIGURE 3 Biophysical analysis of Ca^{2+}-CaM interactions. A, SPR analysis of Ca^{2+} injected over immobilized CaM (left). The affinity was determined by fitting Equation 1 to the steady-state signals extracted from the double-referenced sensorgrams (right). B, MST analysis of fluorescently labeled CaM interaction with Ca^{2+}. Signals from the end of the MST traces (left) were plotted as a function of concentration (right) to determine the affinity using Equation 4. C, UV fluorescence spectroscopy of Ca^{2+}-CaM interaction: normalized intensities for the intrinsic tyrosine fluorescence of CaM ($\lambda_{ex} = 274$ nm, $\lambda_{em} = 304$ nm) were plotted as a function of Ca^{2+} concentration, and the EC_{50} value was determined using Equation 3

2 | RESULTS

2.1 | Biosensor surfaces for CaM interaction studies

Two types of sensor surfaces and experimental designs were used in the present study, one with CaM immobilized and the other with full-lenth Ng (Ng$_{fl}$) immobilized. The CaM surface was used for studies of CaM interactions with Ca^{2+}, CaMKII$_{290-309}$, and Ng$_{27-50}$. It was prepared by immobilizing CaM via amine coupling on SPR biosensor surfaces at surface densities of approximately 400 response units (RU). The Ng$_{fl}$ surface was used for interaction studies between CaM and Ng$_{fl}$. The surface was prepared by capturing Ng$_{fl}$ containing a N-terminal His-tag to antipolyhistidine antibody-coated sensor surfaces. An analysis cycle was then initiated by capturing Ng$_{fl}$ at levels of approximately 300 RU (Figure 2). After a stabilization period, CaM was injected to monitor the interaction. Before a new cycle was started, the antibody surface was completely regenerated by injecting 10 mM glycine, pH 1.5. The surface densities of captured Ng$_{fl}$ varied slightly between the different replicate experiments, but the relative variation in surface

TABLE 1 Affinities for Ca^{2+} interactions with CaM, studied by SPR, MST, and UV fluorescence spectroscopy. Data is presented as the average K_D from the indicated number of replicate experiments (n) and the corresponding standard error (SE)

Method	K_D [M] (n)	T [°C]
SPR	$(3.2\pm0.2) \times 10^{-6}$ (5)	22
SPR	$(2.8\pm0.3) \times 10^{-6}$ (4)	25
MST	$(3.0\pm0.5) \times 10^{-6}$ (4)	25
UV	$(3.1\pm0.2) \times 10^{-6}$* (4)	22

*EC_{50} at total CaM concentration 1 μM, with the slope factor $h = 1.6$

density within a replicate experiment was less than 1%, thereby providing comparable surface properties during the interaction analysis.

2.2 | Validation of CaM interaction studies

Calmodulin interactions with Ca^{2+} and polypeptides were studied by several biophysical methods. The SPR, MST, and UV spectroscopic assays were all set up for analysis of the interaction between CaM and Ca^{2+} to characterize the basic system and validate the methods.

Surface plasmon resonance provided data for the interaction between Ca^{2+} and immobilized CaM, as shown in Figure 3A. The interaction was very rapid, so the association and dissociation rate constants could not be quantified. Steady-state affinity analysis was performed, and the macroscopic K_D was determined to $K_D = 2.8$ μM at 25°C and $K_D = 3.2$ μM at 22°C (Table 1).

The interaction between Ca^{2+} and fluorescently labeled CaM was also analyzed at equilibrium by MST at 25°C (Figure 3B). The affinity was similar, with $K_D = 3.0$ μM (Table 1).

In addition, the interaction between Ca^{2+} and CaM was measured at equilibrium by intrinsic tyrosine fluorescence, illustrated in Figure 3C. Experimental data, obtained at 22°C, were approximated using Equation 3, and the observable affinity was estimated to $EC_{50} = 3.1$ μM at a CaM concentration of 1 μM, with a corresponding slope factor of $h = 1.6$ (Table 1). The determined slope factor of 1.6 indicates positive cooperativity of Ca^{2+} binding to the C-lobe of CaM.

2.3 | Analysis of CaM-CaMKII$_{290-309}$ interactions

Using SPR biosensor analysis, the interaction between CaMKII$_{290-309}$ and immobilized CaM was observed at the presence of Ca^{2+}, while no
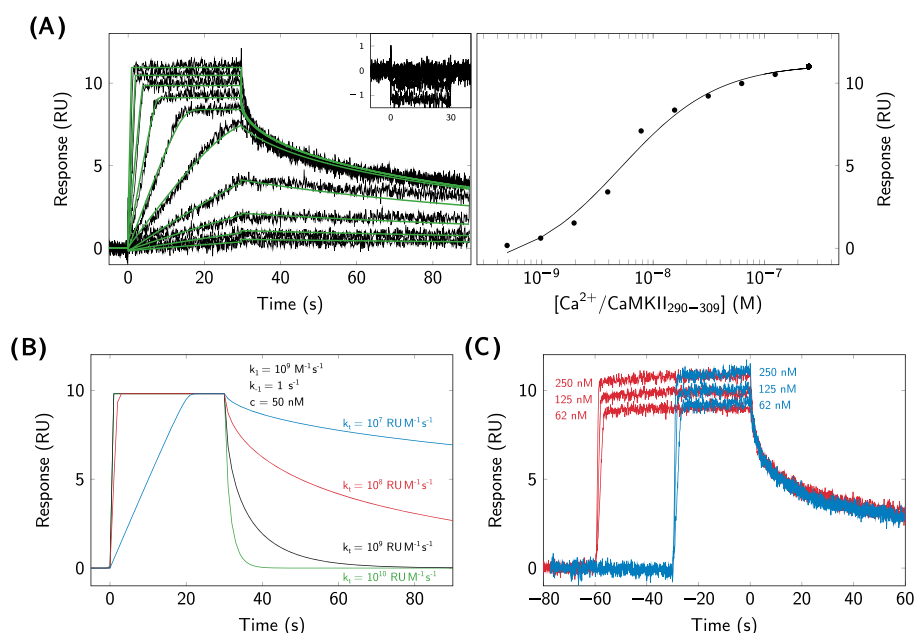

FIGURE 4 Kinetic analysis of CaM-CaMKII$_{290-309}$ interactions. A, CaMKII$_{290-309}$ was injected over immobilized CaM under Ca^{2+}-saturated conditions (left) and Ca^{2+}-depleted conditions (shown in insert, left). A reversible 1-step model (Scheme 1) was fitted to the double-referenced sensorgrams (green solid lines). The affinity was determined by fitting Equation 1 to the steady-signals extracted from the double-referenced sensorgrams (right). B, Simulation of the effect of different values of the mass transport coefficient (k_t) on the kinetics of the CaMKII$_{290-309}$-CaM interaction under Ca^{2+}-saturated conditions. C, Effect of varying injection times (blue: 30 s, red: 60 s) on interactions between CaMKII$_{290-309}$ and CaM under Ca^{2+}-saturated conditions

interaction was detected under Ca^{2+}-depleted conditions. Figure 4A shows sensorgrams under Ca^{2+}-saturated (main graph) and depleted (insert) conditions.

The experimental data could be described by a reversible 1-step model (Scheme 1), and kinetic parameters were very fast, initially approximated to 10^9 M^{-1} s^{-1} for the association rate constant and 1 s^{-1} for the dissociation rate constant. However, the instrument mass transport coefficient was 10^7 RU M^{-1} s^{-1}, which, according to the empirical criterion by Karlsson (Equation 2),[30] is indicative of mass transport–limited kinetic measurements. Simulations using the estimated rate constants and different mass transport coefficient (k_t) showed that the sensorgrams were highly sensitive to variations in k_t values (Figure 4B). Attempts to overcome the mass transport limitation by reducing the amount of immobilized CaM and increasing the flow rate to 90 μL min^{-1} were not successful. The kinetic parameters could therefore not be reliably estimated. For these reasons, the affinity for the CaM-CaMKII$_{290-309}$ interaction ($K_D = 7.1$ nM, Table 2) was determined by steady-state analysis, as shown in Figure 4A.

Despite the difficulties in determining reliable kinetic rate constants, experiments with varying injection times were performed to obtain qualitative information about the interaction mechanism. Figure 4C shows that the sensorgrams from 3 different CaMKII$_{290-309}$ concen-

trations injected for 30 s and 60 s, respectively, overlap very well. This indicates that CaMKII$_{290-309}$ interacts with CaM according to a 1-step model, as shown in Scheme 1.

$$A + B \underset{k_{-1}}{\overset{k_1}{\rightleftharpoons}} AB$$
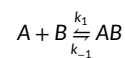
Scheme 1: Reversible 1:1 mechanism for interaction between A and B.

The CaM-CaMKII$_{290-309}$ interaction under Ca^{2+}-saturated conditions was also evaluated by MST analysis, as shown in Figure 5A. The MST-derived affinity was determined to $K_D = 190$ nM, differing more than one order of magnitude from the SPR-derived affinity (Table 2).

2.4 | Analysis of CaM-neurogranin interactions

The interaction between CaM and Ng$_{27-50}$, a peptide containing the CaM-binding site of Ng$_{fl}$ and CaM, was initially studied in a similar manner as in the experiments with CaMKII$_{290-309}$. Surprisingly, the interaction was only detected under Ca^{2+}-saturated conditions (Figure 6A). The relatively weak affinity was determined by steady-state analysis to $K_D = 14$ μM (Table 3). As a control experiment, Ng$_{27-50}$ was immobilized by amine coupling, and CaM was injected as the analyte. Although Ng$_{27-50}$ could be immobilized at high surface densities, theoretically sufficient for detection, an interaction with CaM was not detected (data not shown).

Since the results using Ng$_{27-50}$ were not in accordance with the previous data,[6,8] experiments were performed also with Ng$_{fl}$. For this, Ng$_{fl}$ was immobilized via antipolyhistidine antibody-coated biosensor surfaces by affinity capture, as illustrated in Figure 2. Interactions of Ng$_{fl}$ with CaM were monitored both under Ca^{2+}-depleted (Figure 6B) and Ca^{2+}-saturated conditions (Figure 6C). In the absence of Ca^{2+}, the kinetics of the interaction could be described by a 1-step interaction model (Scheme 1). The association rate constant was determined to

TABLE 2 Affinities for interactions between CaM and CaMKII$_{290-309}$ in the presence (2 mM CaCl$_2$) of and in the absence of calcium. Data are presented as the average value from the indicated number of replicate experiments (n) and the corresponding standard error (SE)

Interaction	K_D^{SPR} [M] (n)	K_D^{MST} [M] (n)
Ca^{2+}/CaM-CaMKII$_{290-309}$	$(7.1 \pm 2.5) \times 10^{-9}$ (5)	$(1.9 \pm 0.7) \times 10^{-7}$ (3)
apoCaM-CaMKII$_{290-309}$	nd (2)	nm

nd - no interaction was detected; nm - not measured

(A)

(B)
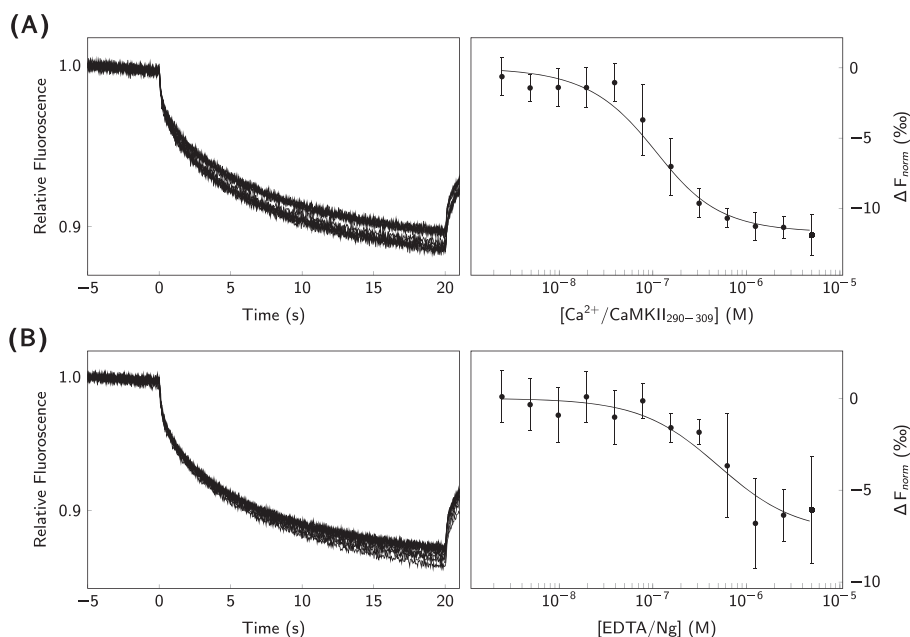
FIGURE 5 MST analysis of CaM-CaMKII$_{290-309}$ and CaM-Ng$_{fl}$ interactions. Thermophoresis of fluorescently labeled CaM was measured over a range CaMKII$_{290-309}$ and Ng$_{fl}$ concentrations. A, CaMKII$_{290-309}$ in Ca^{2+}-saturating conditions; B, Ng$_{fl}$ under Ca^{2+}-depleted conditions. Extracted signals from the end of the Microscale thermophoresis traces were plotted as a function of concentration (black circles), and the affinities were determined by fitting Equation 4 to the data

(A)

(B) **(C)**

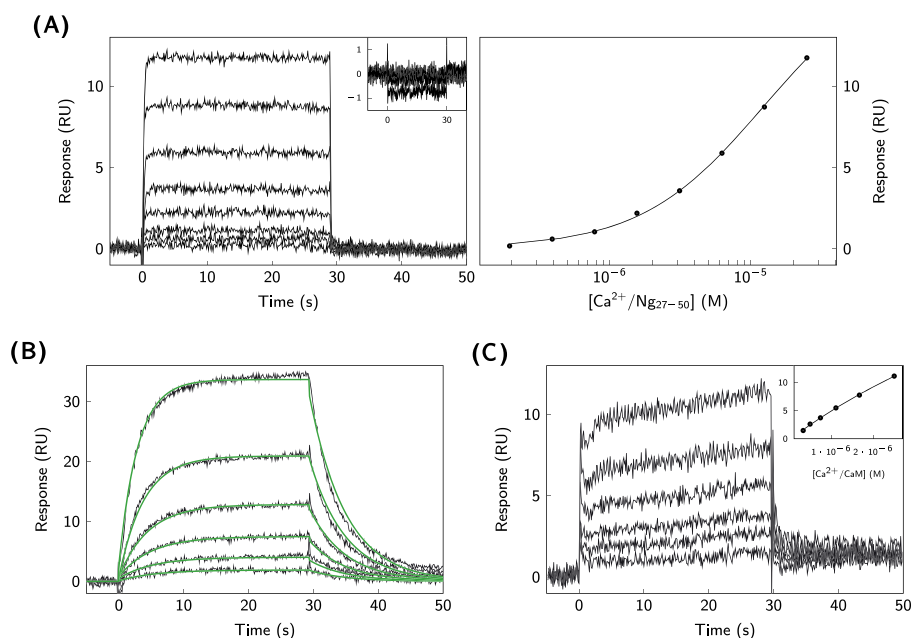**FIGURE 6** SPR analysis of CaM-Ng interactions. A, Ng$_{27-50}$ was injected over immobilized CaM under Ca^{2+}-saturated and Ca^{2+}-depleted (shown in insert) conditions (left). Equation 1 was fitted to the signals extracted from the end of the sensorgrams (right). B, CaM was injected under Ca^{2+}-depleted conditions over affinity captured Ng$_{fl}$, and the kinetics rate constants were determined by fitting a reversible 1-step model according to Scheme 1 (green solid lines). C, CaM was injected over affinity captured Ng$_{fl}$ under Ca^{2+}-saturated conditions, and the affinity was estimated using Equation 1

TABLE 3 Kinetic rate constants and affinities for the interaction between CaM and Ng variants. Data is presented as as the average value from the indicated number of replicate experiments (n) and the corresponding standard error (SE)

Interaction	k_1^{SPR} [M^{-1} s^{-1}]	k_{-1}^{SPR} [s^{-1}]	K_D^{SPR} [M] (n)	K_D^{MST} [M] (n)
Ca^{2+}/CaM-Ng$_{27-50}$	nd	nd	$(1.4\pm0.2) \times 10^{-5}$ (4)	nd (2)
apoCaM-Ng$_{27-50}$	nd	nd	nd (2)	nm
apoCaM-Ng	$(3.4\pm0.2) \times 10^5$	$(1.6\pm0.1) \times 10^{-1}$	$(4.8\pm0.4) \times 10^{-7}$(6)	$(8.9\pm2.5) \times 10^{-7}$ (4)
Ca^{2+}/CaM-Ng	nd	nd	$(1.9\pm0.2) \times 10^{-5}$(5)	nm

nd - parameter was not quantified or no interaction was detected; nm - not measured

$k_1 = 3.4 \times 10^5$ M^{-1} s^{-1} and the dissociation rate constant to $k_{-1} = 1.6 \times 10^{-1}$ s^{-1}, corresponding to an affinity of $K_D = 480$ nM (Table 3). In the presence of Ca^{2+}, higher concentrations of CaM were required to obtain detectable signals, and the kinetic rate constants could not reliably be determined. By using steady-state analysis, the affinity of Ng$_{fl}$ binding to Ca^{2+}-saturated CaM was estimated to $K_D = 19$ μM (Table 3).

The interaction between Ng$_{fl}$ and CaM was further analyzed by MST, and Figure 5B illustrates the MST traces observed upon interaction. The affinity at equilibrium was determined to $K_D = 890$ nM (Table 3). Because of the low affinity between Ng and CaM in the presence of Ca^{2+}, MST analysis would have required impractically high concentrations of Ng and was therefore not performed.

3 | DISCUSSION

The CaM interactome, especially in synapses, is a complex and dynamic network of protein-protein interactions. It is subjected to further modulation by variations of intracellular Ca^{2+} concentrations and by the spatial organization of the different binding partners. Because of its central role in mediating synaptic plasticity of the brain, it is of great interest to improve our understanding of the underlying interactions of CaM. In the present study, we pursued a purely *in vitro* based approach using complementary biophysical methodologies for kinetic and mechanistic interaction studies of two CaMBPs, Ng, and CaMKII. The 2 proteins differ not only in their nature, Ng being a noncatalytic protein of the calpacin family and CaMKII being an enzyme, but more importantly in the Ca^{2+}-dependency of their interactions with CaM. Developing information-rich biophysical assays for studying such diverse proteins, with respect to structure, function, and Ca^{2+}-dependence is an important prerequisite to easily apply the methodology for studies of other CaMBPs.

Surface plasmon resonance biosensor technology is a powerful technique for kinetic studies of biomolecular interactions. The possibility to obtain kinetic information from the real-time data allows one to gain more detailed insights into a given interaction than is provided by equilibrium-based techniques. However, there are some issues that need to be considered in the design of an SPR assay. The preparation of a functional, sensitive, and stable sensor surface is a first critical step.

The most commonly used technique to immobilize proteins onto biosensor surfaces is through amine coupling. This technique involves covalent attachment via primary amine groups of lysine residues in the target protein. This can potentially disturb interactions, especially if the lysine residues are located within the ligand-binding site. Amine coupling was a suitable method for immobilizing CaM but did not result in a functional Ng_{fl} surface. This was most likely due to the location of the majority of lysine residues within the IQ motif and therefore within the binding site for CaM, as shown in Figure 1. Affinity capture using an antibody targeted against the N-terminal His residues of Ng_{fl} was found to be a suitable alternative and allowed the extraction of reliable kinetic information (Figure 2). Analysis of the interactions between Ng_{fl} and immobilized CaM, especially under Ca^{2+}-depleted conditions, provided similar results as with affinity-captured Ng_{fl} (data not shown). However, residual amounts of glycerol from the Ng_{fl} stock gave rise to unwanted secondary effects that disturbed the analysis, especially during experiments under Ca^{2+}-saturated conditions that required higher concentration of Ng_{fl}.

3.1 | Ca^{2+}-CaM interactions studied by orthogonal biophysical assays

In the present study, different aspects of CaM interactions were analyzed. The primary aim was to characterize and compare the kinetics of Ng and CaMKII interactions with Ca^{2+}/CaM and apoCaM. As a first step, the ability to detect how CaM responded to Ca^{2+} concentrations was investigated by using SPR- and MST-based analysis, complemented by fluorescence spectroscopy. For the SPR analysis, CaM was immobilized by amine coupling and the achieved surface density was sufficient to reliably monitor the Ca^{2+} interaction with adequate sensitivity. The macroscopic K_D of 2.8 μM is in agreement with the half maximal concentration of the maximum response ($K_{1/2}$) that has been determined by the use of SPR biosensor analysis in a previous study. [31] From the biosensor analysis, it is not possible to distinguish whether Ca^{2+} binding is measured to an individual lobe of CaM or whether the macroscopic K_D describes the overall affinity to the 4 EF-hands of CaM.

Ca^{2+} interactions with CaM were additionally verified using MST analysis. The labeling chemistry involved in the MST experiments is essentially the same as the immobilization chemistry in the SPR-based experiments, except of the probe nature — fluorescent labeling results in a covalent attachment of a bulky hydrophobic moiety rather than a flexible hydrophilic polymer in SPR experiments. However, MST represents a monophasic system, and the K_D values acquired through the thermophoretic measurements are typically comparable with values obtained using other methods. It was found to be the case also for Ca^{2+} interactions with CaM.

As a further complement to the biosensor and MST analyses, intrinsic tyrosine fluorescence spectroscopy was used. It is sensitive to Ca^{2+} binding to the C-lobe of CaM. [32] The analysis indicated an EC_{50} of 3.1 μM and positive cooperativity of Ca^{2+} binding within the C-lobe of CaM. Thus, the labeling used in SPR and MST analyses did apparently not interfere with Ca^{2+} binding activity of CaM.

In summary, the results from SPR, MST, and UV fluorescence measurements show that neither the immobilization of CaM on biosensor surfaces nor the fluorescent labeling for MST analysis affected the apparent Ca^{2+}-binding properties, suggesting that these methods should provide reliable measurements of CaM interactions with various partners.

3.2 | Qualitative kinetic analysis of CaM-CaMKII$_{290-309}$ interactions

Surface plasmon resonance and MST analysis both demonstrated that Ca^{2+}/CaM binds to CaMKII$_{290-309}$ with nanomolar affinity (Figures 4A and 5A). The SPR-based kinetic measurements showed that the interaction was fast and limited by diffusion of CaMKII$_{290-309}$ to the CaM surface. The sensorgrams contained typical signs of limited mass-transport, including (1) an initial linear association phase, (2) a sharp transition to steady state upon the delayed establishment of an equilibrium at the sensor surface, and (3) an apparently slow dissociation phase caused by rebinding of CaMKII$_{290-309}$ before being washed off from the sensor surface. [33,34] Furthermore, evaluating the approximated kinetic rate constants for the Ca^{2+}/CaM-CaMKII$_{290-309}$ interaction showed that the association rate constant was lower than the mass-transport coefficient, leading to a ratio based on the criterion introduced by Karlsson [30] that by far exceeded the empirically determined ratio of 5. When exceeding this ratio, mass transport effects have a strong effect on the determined parameters and lead to uncertainties in the determination of the kinetic parameters. For this reason, it needs to be emphasized that the apparently slow dissociation of CaMKII$_{290-309}$ shown in Figure 4A does not correspond to the formation of a kinetically stable Ca^{2+}/CaM-CaMKII complex. Simulations performed for the given interaction, using the approximated kinetic rate constants, showed high sensitivity toward variations of the mass transport coefficient, k_t, resulting in rapid kinetics once the effect of k_t on the association rate constant, k_1, became negligible (Figure 4B).

It is worth noting that the interaction could be completely broken up by a short (15 s) injection of HBS-T-EDTA (data not shown). The observed strength of the interaction can thus not be attributed to experimental artifacts due to unspecific binding, analyte precipitation, or other effects that do not correspond to a unspecific molecular recognition. Furthermore, practically identical dissociation curves for different injection times indicated that the interaction was not complex, and it was not meaningful to consider more complicated models than the simple 1-step interaction model shown in 1.

Despite the inability to reliably quantify the kinetic rate constants for the Ca^{2+}/CaM-CaMKII$_{290-309}$ interaction, qualitatively, the analysis provided strong support for a very rapid binding event. This seems to be in agreement with results obtained for the interaction between dansylated CaM and both phosphorylated and unphosphorylated α-CaMKII from the rat brain, where the association rate constants where determined to $k_1 = 1.5 \times 10^8$ M^{-1} s^{-1} and $k_1 = 0.5 \times 10^8$ M^{-1} s^{-1}, respectively. [35]

Steady-state analysis was not affected by the mass-transport limitation, and the affinity was determined to $K_D = 7.1$ nM. This is in agreement with results from fluorescence anisotropy measurements under Ca^{2+}-saturated conditions, where an affinity of less than 10 nM was reported for CaMKII$_{290-309}$ [5] and of $K_D = 45$ nM for unphosphorylated α-CaMKII. [35] It is worth noticing that the affinity and kinetics of CaMKII$_{290-309}$ to Ca^{2+}/CaM, although not fully resolved, seem to be in agreement with those obtained for unphosphorylated α-CaMKII.

Phosphorylated α-CaMKII has a considerably slower dissociation rate constant ($< 1 \times 10^{-3}$ s^{-1}) and therefore an affinity in the low picomolar range.[35]

The affinity for the Ca^{2+}/CaM-CaMKII$_{290-309}$ interaction determined by MST was more than 1 order of magnitude higher (Table 2) than determined with the SPR assay. Such a mismatch between MST- and SPR-derived K_D values for this interaction, under otherwise comparable conditions, might be caused by the introduction of a bulky hydrophobic group of the fluorescent label during the MST analysis, potentially leading to steric hindrance and a reduced affinity for this particular interaction.

In the absence of Ca^{2+}, the interaction of CaMKII$_{290-309}$ with CaM was not detected within the measured concentration range. While the affinity under Ca^{2+}-depleted conditions has been reported to be in the mid micromolar range,[5] determination of such a low affinity of CaMKII$_{290-309}$ to apoCaM was not feasible in the given experimental setup. It would require high micromolar peptide concentrations, which would in turn likely lead to artifacts in the SPR biosensor assay. An affinity for the apoCaM-CaMKII$_{290-309}$ interaction is likely to be 4 to 5 orders of magnitude lower than for the Ca^{2+}/CaM-CaMKII$_{290-309}$. The relevance of such a weak interaction can be regarded as negligible, since CaMKII requires the initial activation by Ca^{2+}/CaM to mediate its physiological effects.

3.3 | Biosensor analysis confirms Ng$_{27-50}$ as a poor model system for full-length neurogranin

When performing biochemical studies using recombinant proteins, a decision has to be made regarding the form of the investigated protein. Truncated proteins are commonly used to reduce the complexity and difficulties associated with studying full-length proteins, like protein stability, solubility, and expression level. This was the case for CaMKII, which, as a wild-type protein presents considerable challenges for *in vitro* biophysical interaction studies because of its size, domain organization, and supramolecular nature. The CaM-binding domain of CaMKII has been mapped to the amino acids 290-309 of the human full-length protein. There is ample experimental data, both from direct interaction studies and competition experiments, showing that CaMKII$_{290-309}$ binds to CaM with low nanomolar affinity and that the interaction practically exclusively occurs in the presence[5,36] of Ca^{2+}. This peptide is capable of substrate-directed inhibition of full-length CaMKII.[36,37] The Ca^{2+}-dependence of the substrate-directed inhibition mimicked the behavior of the full-length protein and the peptide, therefore, it is generally regarded as a valid model system to study the high-affinity interaction between CaM and CaMKII. Furthermore, as discussed in Section 3.2, the binding data obtained for CaMKII$_{290-309}$ seem to be in agreement with results for unphosphorylated CaMKII.

For Ng, the situation regarding the validity of using a truncated protein variant encompassing the IQ domain, which contains the CaM-binding site of Ng, is not as clear as for CaMKII$_{290-309}$. In 2 previous studies,[6,8] the role of the IQ domain of Ng (Ng$_{IQ}$) has been addressed experimentally, but the results were contradictory. In Kumar et al.,[6] the authors conclude that Ng IQ-motif containing peptide can be regarded as a valid model for the full-length protein, while the results

from Hoffman et al.[8] did not agree with this conclusion. The present results give support for concluding that the peptide is not a valid model system for full-length Ng.

While Ng$_{27-50}$ interacted with Ca^{2+}/CaM with micromolar affinity (Table 3), the interaction with apoCaM was not detected. These findings were at first intriguing, especially considering results from ITC analysis reporting nanomolar affinity of Ng$_{27-50}$ to apoCaM and micromolar affinity to Ca^{2+}/CaM.[6] However, in a more recent study, where a similar peptide was used (Ng$_{26-49}$ instead of Ng$_{27-50}$), these results were not confirmed. Instead, fluorescence spectroscopy using Ng$_{26-49}$ indicated positive heterotropic cooperativity for Ca^{2+} binding to CaM, while Ng$_{fl}$ indicated negative heterotropic cooperativity.[8] Furthermore, structural studies using nuclear magnetic resonance have shown that Ng$_{26-49}$ forms contacts with residues of CaM only within the C-lobe, while Ng$_{fl}$ forms contacts both with residues in the C- and N-lobe.[8] Such structural differences can be expected to result in considerable variations of the CaM-binding properties of Ng$_{fl}$ and the derived IQ-motif containing peptide.

In conclusion, the present data from SPR biosensor analysis confirms that Ng$_{27-50}$ is not a suitable model system for Ng$_{fl}$ for studying CaM interactions.

3.4 | Quantitative kinetic analysis of CaM interaction with Ng

Having confirmed that Ng$_{27-50}$ is a poor model system for Ng, kinetic analysis was performed with the full-length protein. As discussed above, for the SPR analysis, Ng$_{fl}$ was immobilized to SPR biosensor surfaces by affinity capture. Calmodulin was injected as analyte in solution both in its apo- and Ca^{2+}-saturated forms.

The influence of Ca^{2+} on the kinetics of the CaM-Ng$_{fl}$ interaction was clearly seen (Figures 6B and 6C). For the apoCaM-Ng$_{fl}$ interaction, both the association and dissociation rate constants could be resolved and corresponded to an affinity of $K_D = 480$ nM (Table 3). There was a strong agreement between the affinity obtained by SPR and MST analysis, thereby supporting the validity of the determined K_D values (Table 3). Under Ca^{2+}-saturated conditions, the kinetic rate constants were too rapid to be determined by SPR analysis, but it was shown that the affinity decreased to approximately $K_D = 19$ µM.

Compared with previous analysis on the CaM-Ng$_{fl}$ interaction, there is a good agreement of the present SPR- and MST-based results with previous ITC-based results[8]. In the presence of 150 mM potassium chloride (KCl), the affinity of the apoCaM-Ng$_{fl}$ interaction of $K_D = 480$ nM, as determined by SPR and MST, is in good agreement with the affinity of $K_D = 800$ nM determined by ITC.[8] The interaction of Ng$_{fl}$ with Ca^{2+}/CaM could previously not be resolved in the presence of 150 mM KCl[8]; therefore, a valid comparison with the present data cannot be made. However, on a qualitative level, previous results obtained with varying KCl concentrations showed a consistently higher affinity of Ng$_{fl}$ to apoCaM than to Ca^{2+}/CaM,[8] which was observed in the current study as well. Minor differences in measured affinities between the 2 different studies might be caused by differences in the primary structure of the protein constructs used. In Hoffman et al.,[8] human Ng$_{fl}$ was used containing a D2A point mutation. We used wild-type human Ng$_{fl}$

containing an N-terminal His-tag in the present study. It should therefore be noted that, while there are differences in the absolute affinities in studies on the Ng-CaM interactions, there is strong agreement on the qualitative level that Ng_{fl} interacts with CaM with reasonable affinity both under Ca^{2+}-saturated and Ca^{2+}-depleted conditions.

3.5 | Role of bimodal neurogranin interaction with apo and Ca^{2+}/CaM

Based on the present and previous binding data, [8] it is clear that Ng binds with reasonable affinity to CaM both under Ca^{2+}-depleted and Ca^{2+}-saturated conditions. Other proteins, like CaMKII and AKAP79, whose interaction with CaM that we recently studied using similar methodology,[25] have a clear preference for Ca^{2+}/CaM. This ability might reflect the physiological role of Ng in targeting and concentrating CaM at postsynaptic dendrites [18] that has been described as being a biochemical "capacitor" that releases Ca^{2+}/CaM either gradually or rapid in response to the strength and duration of Ca^{2+} pulses. [38] Under Ca^{2+}-depleted conditions, Ng is the predominant postsynaptic protein that binds apoCaM.[18,39] The relatively slow kinetics of the apoCaM-Ng interaction and the accompanying middle nanomolar affinity are sufficient to target apoCaM and increase its availability for Ca^{2+}/CaM signaling. It has been observed that CaM has a high level of mobility within dendritic spines, [18] and if the CaM-Ng complex would immediately dissociate upon an increase in Ca^{2+} concentration, as previously suggested,[38] CaM could potentially diffuse from the postsynaptic dendrites. This would render the initial concentration of CaM within the dendrites unnecessary. Instead, by having a low affinity in the micromolar range, Ng is able to hold CaM in place until it is competed out by other CaMBPs, for instance CaMKII or AKAP79, that have faster association rate constants and affinities than Ng.[25,35]

4 | CONCLUSIONS

The current project has demonstrated how a biophysical strategy can be applied to elucidate the dynamic details of the calmodulin interactome and its regulation via Ca^{2+}. By studying the interactions of the isolated components directly and using a combination of real-time and equilibrium-based techniques in solution and on sensor surfaces, it was possible to extract details of the interactions. This has revealed distinctive features of the interactions between 2 proteins that interact with CaM in the apo form and the Ca^{2+}-bound form. Specifically, it adds a further dimension to the understanding of how Ng regulates CaM dynamics in synapses.

5 | MATERIALS AND METHODS

5.1 | Proteins and peptides

Calmodulin from the human brain was purchased from Genway Biotech Inc. (San Diego, California), and recombinant bovine CaM was purchased from Merck Millipore (Billerica, Massachusetts). The human and bovine orthologs are structurally identical. Full-length

recombinant human Ng (Ng_{fl}, aa 1–78) with a His-tag at the N-terminus was purchased from Acris Antibodies (Herford, Germany). The IQ-motif containing peptide of Ng (Ng_{27-50}) and a peptide corresponding to the CaM-binding region of CaMKIIα ($CaMKII_{290-309}$) were purchased from Bachem (Bubendorf, Switzerland). An antipolyhistidine antibody was purchased from R&D Systems (Minneapolis, Minnesota). The amino acid sequences of the peptides and proteins used in the experiments are shown in Figure 1.

5.2 | Surface plasmon resonance biosensor-based interaction studies

Surface plasmon resonance (SPR) biosensor-based interaction studies were performed on a Biacore S51 instrument using CM5 sensor chips (GE Healthcare, Uppsala, Sweden). For the interaction studies, sensor surfaces were prepared by immobilizing CaM or Ng.

Calmodulin was immobilized by amine coupling at a temperature of 25°C using a running buffer consisting of 10 mM HEPES, 150 mM NaCl, 0.05% Tween-20, pH 7.4 (HBS-T). The surface was activated by injecting 200 mM 1-ethyl-3-(3-dimethylaminopropyl)carbodiimide hydrochloride (EDC) and 50 mM N-hydroxysuccinimide (NHS) (10 min, 20 μL min^{-1}), followed by injecting 50 μg mL^{-1} CaM (diluted into 10 mM Na-acetate, pH 4.0 (GE Healthcare)) for 20 min (2 μL min^{-1}). The surface was deactivated by injecting 1 M ethanolamine, pH 8.5 (7 min, 25 μL min^{-1}).

Full-length neurogranin was immobilized by affinity capture via the N-terminal His-tag. The antipolyhistidine antibody was first immobilized by amine coupling at a concentration of 10 μg mL^{-1} (diluted into 10 mM Na-acetate, pH 5.5, 10 min injection, 5 μL min^{-1}). Subsequently, Ng_{fl}, diluted to 25 μg mL^{-1} in either HBS-T-EDTA (HBS-T supplemented with 1 mM EDTA) or HBS-T-CaCl$_2$ (HBS-T supplemented with 2 mM CaCl$_2$), was injected over the antibody surface (2 min, 10 μL min^{-1}). During the experiments, the surface was regenerated after every injection of CaM by two 20 s pulses of 10 mM glycine, pH 1.5 (30 μL min^{-1}).

Ca^{2+} interactions were measured at both 25°C and 22°C using HBS-T as running and sample buffer. Ca^{2+} was injected in 2-fold concentration series (200 nM – 50 μM) for 30 s at a flow rate of 90 μL min^{-1}. Interaction studies of $CaMKII_{290-309}$ and Ng_{27-50} with immobilized CaM were performed at 25°C both in the presence (HBS-T-CaCl$_2$) and absence of Ca^{2+} (HBS-T-EDTA). $CaMKII_{290-309}$ (0.5 nM – 250 nM) and Ng_{27-50} (200 nM – 25 μM) were injected in 2-fold concentration series for 30 s at a flow rate of 90 μL.

Calmodulin interactions with immobilized Ng_{fl} were studied at 25°C at a flow rate of 30 μL min^{-1}. Calmodulin was injected for 30 s in 2-fold dilution series (250 nM – 8 nM) in HBS-T-EDTA and in 1.5-fold dilution series (2.5 μM – 300 nM) in HBS-T-CaCl$_2$.

Experimental data was double-referenced by subtracting the response from an untreated reference surface and the average response from 2 blank samples. Biacore T200 Evaluation v1.0 Software (GE Healthcare) was used for steady-state and kinetic analysis. For the steady-state analysis, average signals from a 5 s interval were extracted from the end of the association phase of the sensorgrams and analyzed as a function of ligand concentration using Equation 1. The parameters for the responses when saturation is reached, R_{max}, and for the offset, m, were fitted locally, while the K_D was fitted as a global parameter, $[L]$ corresponds to the ligand concentration.

$$R = \frac{R_{max} \times [L]}{[L] + K_D} + m \qquad (1)$$

For kinetic analysis, a 1:1 interaction model (Scheme 1) was globally fitted to the double-referenced data to determine the association rate constant, k_1, the dissociation rate constant, k_{-1}, and the corresponding K_D value.

The effect of limited mass-transport on kinetic measurements was evaluated using Equation 2 introduced in Karlsson.[30] Simulation of the influence of different values of mass-transport coefficient, k_t, on the kinetics of CaMKII$_{290-309}$ was performed using BIAevaluation v3.0.2 (GE Healthcare).

$$\frac{R_{max} \times k_{on}}{k_t} < 5 \qquad (2)$$

5.3 | Ultraviolet fluorescence spectroscopy

Fluorescence measurements were performed on a Fluoromax-4 Spectrofluorometer (Horiba, Kyoto, Japan) at 22°C using a 0.5 mL 4-side polished quartz cuvette (Hellma Analytics, Müllheim, Germany) with a 10 mm light path. Intrinsic tyrosine fluorescence of CaM was measured at an excitation wavelength of $\lambda_{ex} = 274$ nm and an emission wavelength of $\lambda_{em} = 304$ nm using slit widths of 1 nm and 10 nm, respectively.

Two-fold serial dilutions of Ca^{2+} starting from 40 mM $CaCl_2$ in CaM stock solution (10 mM HEPES, 150 mM NaCl, 10 μM (micromoles) apoCaM, pH 7.4) were prepared. For determination of the Ca^{2+} affinity, 5 μL aliquots from each dilution point were titrated into CaM stock solution.

Fluorescence intensities within every titration series were normalized to span a range from 0 to 1. Equation 3 was fitted to the data using nonlinear regression in the BIAevaluation software 3.0.2. F_{min} and F_{max} correspond to the normalized fluoresence intensity of Ca^{2+}-free and Ca^{2+}-saturated CaM, respectively, EC_{50} to the observable K_D at the given protein concentration, $[Ca^{2+}]$, to the total Ca^{2+} concentration, and h to the slope factor that indicates degree of the binding cooperativity.

$$F = (F_{max} - F_{min}) \times \frac{[Ca^{2+}]^h}{EC_{50}^{\ h} + [Ca^{2+}]^h} + F_{min} \qquad (3)$$

5.4 | Affinity analysis using microscale thermophoresis

Microscale thermophoresis–based interaction analysis was performed on a Monolith NT. Automated MST instrument (NanoTemper Technologies GmbH, Munich, Germany) using standard treated AK002 capillaries at a temperature of 25°C. Excitation and MST power were set to 20%. The initial state was recorded for 5 s, thermophoresis for 20 s and the back diffusion for 1 s.

For MST experiments, CaM was labeled with Cyanine5 NHS-activated ester (Lumiprobe GmbH, Hannover, Germany). The dye was dissolved in 100% dimethyl sulfoxide to a final concentration of 540 μM, and the labeling reaction was performed by incubating 2.5 μM of CaM and 5 μM of the fluorophore in HBS-T supplemented with 1% dimethyl sulfoxide for 30 min at room temperature in the dark. The reaction was stopped by buffer exchange to HBS-T using spin desalting columns with a molecular weight cutoff of 7 kDa (Thermo Scientific, Rockford, USA) according to the instructions of the manufacturer.

Thermophoretic measurements were performed at a constant CaM concentration of 75 nM. Ligands were prepared in 2-fold dilution series (concentrations specified under Results). Interaction of Ca^{2+} with CaM was analyzed in HBS-T, CaMKII$_{290-309}$ with CaM in HBS-T-CaCl$_2$. Analysis of the interaction between apoCaM and Ng$_{fl}$ was performed in HBS-T-EDTA. Data from at least 3 independent replicate experiments were analyzed using the NTAnalysis software (NanoTemper GmbH). The macroscopic dissociation constant (K_D) was determined using Equation 4:

$$\frac{[BL]}{[B_0]} = \frac{([L_0] + [B_0] + K_D) - \sqrt{([L_0] + [B_0] + K_D)^2 - 4 \times [L_0] \times [B_0]}}{2 \times [B_0]}, \qquad (4)$$

where $[B_0]$ corresponds to the total concentration of target binding sites, $[L_0]$ to the concentration of titrated ligand, and $[BL]$ to the concentration of formed complex between ligand and target binding sites.[27]

REFERENCES

1. Xia Z, Storm DR. The role of calmodulin as a signal integrator for synaptic plasticity. *Nat Rev Neurosci*. 2005;6(4):267–276.

2. Babu YS, Bugg CE, Cook WJ. Structure of calmodulin refined at 2.2 – resolution. *J Mol Biol*. 1988;204(1):191–204.

3. Kuboniwa H, Tjandra N, Grzesiek S, Ren H, Klee CB, Bax Ad. Solution structure of calcium-free calmodulin. *Nat Struct Biol*. 1995;2(9): 768–776.

4. LaPorte DC, Wierman BM, Storm DR. Calcium-induced exposure of a hydrophobic surface on calmodulin *Biochemistry*. 1980;19(16): 3814–3819.

5. Evans T, Shea MA. Energetics of calmodulin domain interactions with the calmodulin binding domain of CaMKII. *Proteins: Structure, Function, and Bioinformatics*. 2009;76(1):47–61.

6. Kumar V, Chichili VPR, Zhong L, et al. Structural basis for the interaction of unstructured neuron specific substrates neuromodulin and neurogranin with calmodulin. *Sci Rep*. 2013;3:1392.

7. Baudier J, Deloulme JCh, Van Dorsselaer A, Black D, Matthes HW. Purification and characterization of a brain-specific protein kinase C substrate, neurogranin (p17). Identification of a consensus amino acid sequence between neurogranin and neuromodulin (gap43) that corresponds to the protein kinase C phosphorylation site and the calmodulin-binding domain. *J Biol Chem*. 1991;266(1):229–237.

8. Hoffman L, Chandrasekar A, Wang X, Putkey JA, Waxham MN. Neurogranin alters the structure and calcium binding properties of calmodulin. *J Biol Chem*. 2014;289(21):14644–14655.

9. Lisman J, Schulman H, Cline H. The molecular basis of CaMKII function in synaptic and behavioural memory. *Nat Rev Neurosci*. 2002;3(3):175–190.

10. Hunter T, Schulman H. CaMKII structure - an elegant design. *Cell*. 2005;123(5):765–767.

11. Brocke L, Chiang LW, Wagner PD, Schulman H. Functional implications of the subunit composition of neuronal CaM kinase II. *J Biol Chem.* 1999;274(32):22713–22722.

12. Erondu NE, Kennedy MB. Regional distribution of type II Ca^{2+}/calmodulin-dependent protein kinase in rat brain. *The J Neurosci.* 1985;5(12):3270–3277.

13. Derkach V, Barria A, Soderling TR. Ca^{2+}/calmodulin-kinase II enhances channel conductance of α-amino-3-hydroxy-5-methyl-4-isoxazolepropionate type glutamate receptors. *Proceedings of the National Academy of Sciences.* 1999;96(6):3269–3274.

14. Lai Y, Nairn AC, Greengard P. Autophosphorylation reversibly regulates the Ca^{2+}/calmodulin-dependence of Ca^{2+}/calmodulin-dependent protein kinase II. *Proceedings of the National Academy of Sciences.* 1986;83(12):4253–4257.

15. Gerendasy DD, Sutcliffe JG. Rc3/neurogranin, a postsynaptic calpacitin for setting the response threshold to calcium influxes. *Mol Neurobiol.* 1997;15(2):131–163.

16. Rhoads AR, Friedberg F. Sequence motifs for calmodulin recognition. *The FASEB Journal.* 1997;11(5):331–340.

17. Zhong L, Cherry T, Bies CE, Florence MA, Gerges NZ. Neurogranin enhances synaptic strength through its interaction with calmodulin. *The EMBO Journal.* 2009;28(19):3027–3039.

18. Petersen A, Gerges NZ. Neurogranin regulates cam dynamics at dendritic spines. *Sci Rep.* 2015;5:11135.

19. Keller CH, Olwin BB, LaPorte DC, Storm DR. Determination of the free-energy coupling for binding of calcium ion and troponin I to calmodulin. *Biochemistry.* 1982;21(1):156–162.

20. Olwin BB, Storm DR. Calcium binding to complexes of calmodulin and calmodulin binding proteins. *Biochemistry.* 1985;24(27):8081–8086.

21. Gaertner TR, Putkey JA, Waxham MN. Rc3/neurogranin and Ca^{2+}/calmodulin-dependent protein kinase II produce opposing effects on the affinity of calmodulin for calcium. *J Biol Chem.* 2004;279(38):39374–39382.

22. Lai M, Brun D, Edelstein SJ, Le Novère N. Modulation of calmodulin lobes by different targets: an allosteric model with hemiconcerted conformational transitions. *PLoS Computational Biology.* 2015;11(1):e1004063.

23. Monod J, Wyman J, Changeux J-P. On the nature of allosteric transitions: a plausible model. *J Mol Biol.* 1965;12(1):88–118.

24. Gorny X, Mikhaylova M, Seeger C, Reddy PP, Reissner C, Schott BH, Danielson UH, Kreutz MR, Seidenbecher Constanze. AKAP79/150 interacts with the neuronal calcium-binding protein caldendrin. *J Neurochem.* 2012;122(4):714–726.

25. Seeger C, Gorny X, Reddy PP, Seidenbecher C, Danielson UH. Kinetic and mechanistic differences in the interactions between caldendrin and calmodulin with AKAP79 suggest different roles in synaptic function. *J Mol Recognit.* 2012;25(10):495–503.

26. Duhr S, Braun D. Why molecules move along a temperature gradient. *Proceedings of the National Academy of Sciences.* 2006;103(52):19678–19682.

27. Wienken CJ, Baaske P, Rothbauer U, Braun D, Duhr S. Protein-binding assays in biological liquids using microscale thermophoresis. *Nat Commun.* 2010;1:100.

28. Dedman JR, Potter JD, Jackson RL, Johnson JD, Means AR. Physicochemical properties of rat testis Ca^{2+}-dependent regulator protein of cyclic nucleotide phosphodiesterase. *J Biol Chem.* 1977;252:8415–8422.

29. Pundak S, Roche RS. Tyrosine and tyrosinate fluorescence of bovine testes calmodulin: calcium and pH dependence. *Biochemistry.* 1984;23(7):1549–1555.

30. Karlsson R. Affinity analysis of non-steady-state data obtained under mass transport limited conditions using BIAcore technology. *J Mol Recognit.* 1999;12(5):285–292.

31. Dell'Orco D, Sulmann S, Linse S, Koch K-W. Dynamics of conformational Ca^{2+}-switches in signaling networks detected by a planar plasmonic device. *Anal Chem.* 2012;84(6):2982–2989.

32. Richman PG, Klee CB. Specific perturbation by Ca^{2+} of tyrosyl residue 138 of calmodulin. *J Biol Chem.* 1979;254(12):5372–5376.

33. Schuck P. Kinetics of ligand binding to receptor immobilized in a polymer matrix, as detected with an evanescent wave biosensor. I. A computer simulation of the influence of mass transport. *Biophys J.* 1996;70(3):1230–1249.

34. Nico J, Plomp E, Fischer MJE, Ruijtenbeek R. Kinetic analysis of the mass transport limited interaction between the tyrosine kinase lck SH2 domain and a phosphorylated peptide studied by a new cuvette-based surface plasmon resonance instrument. *Anal Biochem.* 2000;279(1):61–70.

35. Meyer T, Hanson PI, Stryer L, Schulman H. Calmodulin trapping by calcium-calmodulin-dependent protein kinase. *Science.* 1992;256(5060):1199–1202.

36. Payne ME, Fong YL, Ono T, Colbran RJ, Kemp BE, Soderling TR, Means AR. Calcium/calmodulin-dependent protein kinase II. characterization of distinct calmodulin binding and inhibitory domains. *J Biol Chem.* 1988;263(15):7190–7195.

37. Colbran RJ, Schworer CM, Hashimoto Y, Fong YL, Rich DP, Smith MK, Soderling TR. Calcium/calmodulin-dependent protein kinase II. *Biochem J.* 1989;258(2):313–325.

38. Gerendasy DD, Herron SR, Watson JB, Sutcliffe JG. Mutational and biophysical studies suggest RC3/neurogranin regulates calmodulin availability. *J Biol Chem.* 1994;269(35):22420–22426.

39. Zhabotinsky AM, Camp RN, Epstein IR, Lisman JE. Role of the neurogranin concentrated in spines in the induction of long-term potentiation. *The J Neurosci.* 2006;26(28):7337–7347.